© 2017. Published by The Company of Biologists Ltd | Development (2017) 144, 3430-3439 doi:10.1242/dev.150284

Spermatogonial kinetics in humans

Sara Di Persio[1], Rossana Saracino[1], Stefania Fera[1], Barbara Muciaccia[1], Valentina Esposito[1], Carla Boitani[1], Bartolomeo P. Berloco[2], Francesco Nudo[2], Gustavo Spadetta[3], Mario Stefanini[1], Dirk G. de Rooij[1,*,‡] and Elena Vicini[1,*,‡]

ABSTRACT

The human spermatogonial compartment is essential for daily production of millions of sperm. Despite this crucial role, the molecular signature, kinetic behavior and regulation of human spermatogonia are poorly understood. Using human testis biopsies with normal spermatogenesis and by studying marker protein expression, we have identified for the first time different subpopulations of spermatogonia. MAGE-A4 marks all spermatogonia, KIT marks all B spermatogonia and UCLH1 all Apale-dark (Ap-d) spermatogonia. We suggest that at the start of the spermatogenic lineage there are Ap-d spermatogonia that are GFRA1^{High}, likely including the spermatogonial stem cells. Next, UTF1 becomes expressed, cells become quiescent and GFRA1 expression decreases. Finally, GFRA1 expression is lost and subsequently cells differentiate into B spermatogonia, losing UTF1 and acquiring KIT expression. Strikingly, most human Ap-d spermatogonia are out of the cell cycle and even differentiating type B spermatogonial proliferation is restricted. A novel scheme for human spermatogonial development is proposed that will facilitate further research in this field, the understanding of cases of infertility and the development of methods to increase sperm output.

KEY WORDS: Human, Spermatogonia, GFRA1, UTF1, KIT, UCL-H1, Stem cell renewal, Spermatogonial differentiation

INTRODUCTION

Although extensive studies have yielded considerable information about spermatogenesis in non-primate mammals, our understanding of this process in primates and especially in humans is still scant. In both primates and non-primates, at the start of spermatogenesis there are so-called undifferentiated spermatogonia. In non-primates, this compartment consists of single spermatogonia (A_s), and pairs (A_{pr}) and chains (A_{al}) of spermatogonia. The spermatogonial stem cells (SSCs) are among the A_s spermatogonia (Aloisio et al., 2014; Chan et al., 2014; de Rooij and Russell, 2000; Helsel et al., 2017; Komai et al., 2014; Oatley et al., 2011). In primates, this compartment consists of Apale (Ap) and Adark (Ad) spermatogonia. The Ap spermatogonial nuclei stain lightly and evenly with Hematoxylin, and the Ad nuclei stain darkly and, in humans, show a non-staining rarefaction zone in the middle of the nucleus. Intriguingly, the Ad spermatogonia do not or rarely incorporate S phase markers such as ^{3}H-thymidine or BrdU (Clermont, 1966a,b, 1969; Clermont and Antar, 1973; Simorangkir et al., 2009), and are therefore considered to be quiescent. Several opinions exist as to the function of the Ap and Ad spermatogonia: (1) the Ad spermatogonia are the true stem cells that slowly produce Ap spermatogonia that would not have enough self-renewal capacity to maintain their numbers (Clermont, 1966a,b; Ehmcke et al., 2006); (2) the Ap spermatogonia are the SSCs as they produce differentiating spermatogonia, maintain themselves and produce quiescent Ad spermatogonia that, if Ap spermatogonia are lost, can convert into Ap spermatogonia again (Clermont, 1966a,b; Ehmcke and Schlatt, 2006; Hermann et al., 2010; van Alphen et al., 1988); (3) Ap and Ad are similar cells but in different phases of the cell cycle (Fouquet and Dadoune, 1986; Hermann et al., 2009, 2010).

In most monkey species and non-primate mammals, whole stretches of seminiferous tubules are in the same stage of the cycle of the seminiferous epithelium and subsequent stages follow sequentially along the length of the tubule. In contrast, in the human the epithelial stages occupy only small areas of the tubule basal lamina, and neighboring areas are in randomly different epithelial stages (Johnson, 1994). The reason for this difference is supposed to be related to spermatogonial behavior.

Using testis material from human organ donors, we studied the proliferative activity and differentiation of human spermatogonial cell types to understand the seemingly large differences between human and non-primate spermatogenesis. The expression patterns of GFRA1, UCH-L1, KIT and UTF1 allowed us to distinguish spermatogonial subtypes and the expression of KI67 gave us information about the proliferative activity of these cell types. We established the clonal sizes of Ap and B spermatogonia, and the number of generations of B spermatogonia. A novel concept of human spermatogonial proliferation is proposed. This new view on human spermatogonial behavior will greatly facilitate attempts to better understand abnormal spermatogenesis present in male infertility.

RESULTS

Characterization of human spermatogonia

In rodents, great progress was made by characterizing spermatogonial cell types in whole mounts of seminiferous tubules stained with Hematoxylin. Application of this technique to human seminiferous tubules demonstrated clearly recognizable Ap and Ad spermatogonia (Clermont, 1966b). However, often these cells had an intermediate morphology. For example, some cells had nuclei that stained lightly with Hematoxylin as Ap, but had a nuclear rarefaction zone characteristic of Ad spermatogonial nuclei (Fig. 1A). In particular, in whole mounts, in which the whole nucleus is visible, it is often too difficult to distinguish Ap and Ad spermatogonia, suggesting a gradual transition from Ap to Ad spermatogonia and/or vice versa. In addition the morphological

[1]Fondazione Pasteur Cenci Bolognetti, Department of Anatomical, Histological, Forensic and Orthopaedic Sciences – Section of Histology and Medical Embryology, Sapienza University of Rome, Rome 00161, Italy. [2]Department of General and Specialistic Surgery 'Paride Stefanini', Sapienza University of Rome, Rome 00161, Italy. [3]Department of Cardiovascular, Respiratory, Nephrological, Anesthesiological and Geriatric Sciences, Sapienza University of Rome, Rome 00161, Italy.
*These authors contributed equally to this work

‡Authors for correspondence (elena.vicini@uniroma1.it; d.g.derooij@uu.nl)

C.B., 0000-0002-8452-8907; B.P.B., 0000-0001-9086-0730; M.S., 0000-0002-0637-7322; D.G.d.R., 0000-0003-3932-4419; E.V., 0000-0003-0399-0145

Received 6 February 2017; Accepted 15 August 2017

Development (2017) 144, 3430-3439 doi:10.1242/dev.150284

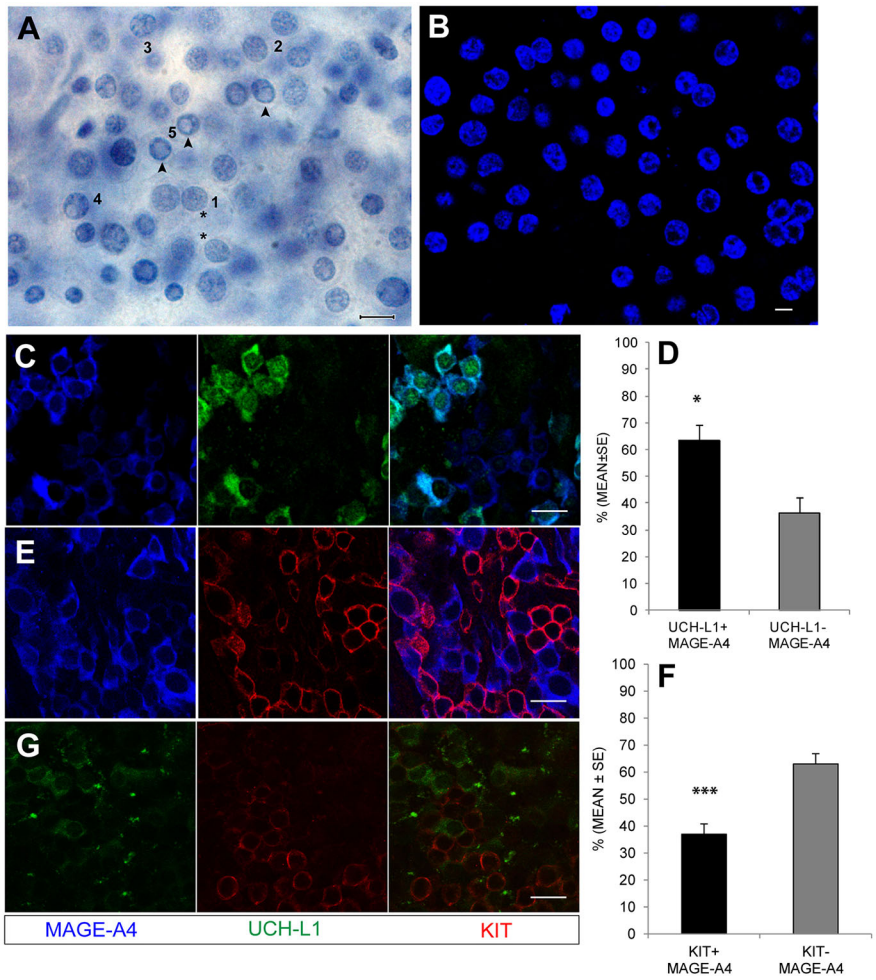

Fig. 1. Characterization of human spermatogonia. (A) View of the cells on the basal lamina of a human seminiferous tubule stained lightly with Hematoxylin. Note the high density of spermatogonia and the variability of their morphology. Cells can be seen that are clearly Ap (asterisks) and Ad (arrowheads) spermatogonia. However, there are many nuclei with an intermediate morphology. Indeed, there may be a transition from Ap to Ad (follow the numbers 1 to 5). Intact seminiferous tubules were formalin fixed and lightly stained with hematoxylin. Scale bar: 8 µm. (B) Cells on the basal lamina of an intact human seminiferous tubule stained with a fluorescent dye for nuclear DNA. Note that no distinction can be made between Ap and Ad spermatogonia. Scale bar: 8 µm (C,E,G) Representative images of intact seminiferous tubules stained for UCH-L1 and MAGE-A4 (C), MAGE-A4 and KIT (E), and UCH-L1 and KIT (G). Scale bars: 20 µm. (D,F) Quantification of the relative proportion of Ap-d (UCH-L1$^+$/MAGE-A4$^+$) and B (KIT$^+$/MAGE-A4$^+$) spermatogonia. (D) 1963 UCH-L1$^+$/MAGE-A4$^+$ cells were scored in three samples. (F) 3315 KIT$^+$/MAGEA-A4$^+$ cells were scored in four samples. *P<0.05, ***P<0.001 (Student's t-test).

analysis of fluorescent-stained nuclei does not allow a clear distinction between Ap and Ad spermatogonia (Fig. 1B). Because of this and because, to date, the specific function of Ap and Ad spermatogonia has remained unclear, we decided to no longer distinguish between Ap and Ad spermatogonia and to use the term Ap-d to indicate the total population of Ap and Ad spermatogonia. A further complication in spermatogonial recognition in humans is that specific fixation methods are required to distinguish B from Ap-d spermatogonia (Clermont, 1966b; Rowley and Heller, 1971).

Spermatogonial density on the basal lamina of human seminiferous tubules is high. Solid packs of KIT$^-$ Ap-d spermatogonia, of KIT$^+$ B spermatogonia or mixtures of these cell types can be seen (Fig. S1). Indeed, human spermatogonial density is so high that the nuclei of the Sertoli cells moved to the second layer of cells above the basal lamina (Fig. S1). It proved to be impossible to discern individual clones of spermatogonia, connected by intercellular bridges, as in rodents (de Rooij, 1973; Huckins, 1971; Lok et al., 1982).

We decided to use marker proteins to distinguish human spermatogonial cell types. To identify Ap-d and B spermatogonia we used MAGE-A4, UCH-L1 and KIT. MAGE-A4 is expressed in all types of spermatogonia (Aubry et al., 2001), UCH-L1 is expressed in Ad-p spermatogonia (Tokunaga et al., 1999a,b), while KIT is specifically expressed in differentiating type spermatogonia (Schrans-Stassen et al., 1999). In prepubertal monkey testes that contain only Ap-d spermatogonia, no KIT staining was found (Hermann et al., 2009). Whole mounts of seminiferous tubules were immunofluorescently stained for MAGE-A4 and UCH-L1 (Fig. 1C) or MAGE-A4 and KIT (Fig. 1E). UCH-L1 and KIT expression did not overlap, with only few spermatogonia weakly expressing UCHL-1 also weakly stained for KIT (Fig. 1G). Using these markers, UCH-L1$^+$ /KIT$^-$/MAGE-A4$^+$ cells represent the Ap-d spermatogonia and the UCH-L1$^-$/KIT$^+$/MAGE-A4$^+$ cells represent the B spermatogonia. We found that 37±4% of the MAGE-A4$^+$ cells were KIT$^+$ and therefore B spermatogonia and 63±6% of the MAGE-A4 were UCH-L1$^+$ and therefore Ap-d spermatogonia (Fig. 1D,F). MAGE-A4 expression was weaker in B than in Ap-d spermatogonia, and was absent in preleptotene spermatocytes (Fig. S2).

Expression of GFRA1 and UTF1 in Ap-d spermatogonia

We next analyzed expression of selected markers within the population of Ap-d by double or triple immunostaining for MAGE-A4 and/or UCH-L1. GFRA1 is a co-receptor for GDNF: a growth factor produced by Sertoli cells and peritubular cells (Singh et al., 2017; Spinnler et al., 2010) that regulates self-renewal and differentiation of murine SSCs, and stimulates the proliferative activity of undifferentiated spermatogonia. GFRA1 is a consensus marker for early undifferentiated spermatogonia, including SSCs (Meng et al., 2000), and is heterogeneously expressed in human Ad and Ap spermatogonia (Grisanti et al., 2009). KIT and GFRA1 double staining revealed no double-positive cells (data not shown), indicating that B spermatogonia do not express GFRA1. By double immunostaining for MAGE-A4 and GFRA1, we found that GFRA1 is expressed in 54±8% of all spermatogonia (Fig. 2A,B) and in 87±

Development (2017) 144, 3430-3439 doi:10.1242/dev.150284

2% of the Ap-d spermatogonia by double immunostaining for UCH-L1 and GFRA1 (Fig. S3A).

UTF1 is a stably chromatin-associated, transcriptional repressor protein that is expressed in Ap-d spermatogonia (von Kopylow et al., 2010, 2012). It is involved in the regulation of differentiation of ES and EC cells (Lin et al., 2012; van den Boom et al., 2007). UTF1 was expressed in 43±3% (Fig. 2C,D) of total spermatogonia and in 56±4% of the Ap-d spermatogonia (Fig. S3B). A few B spermatogonia weakly expressing KIT also weakly stained for UTF1 (Fig. 2E). We conclude that UTF1 is expressed in many Ap-d spermatogonia and in only a few B spermatogonia.

Since both GFRA1 and UTF1 are expressed in many Ap-d spermatogonia, this indicates that they are co-expressed in some Ap-d spermatogonia. In whole mounts stained for MAGE-A4, GFRA1 and UTF1, we found that 38±5% of the spermatogonia were GFRA1^{+}, 17±5% were UTF1^{+} and 25±8% of the cells were double positive for GFRA1 and UTF1 (Fig. 2F,G). Similar results were obtained in whole mounts stained for UCH-L1, GFRA1 and UTF1 (Fig. S3C). Interestingly, we observed a clear difference in expression levels of GFRA1 in UTF1-positive and -negative spermatogonia (Fig. 2F). Quantifying the fluorescence intensity of GFRA1 in the two subsets revealed that the level of GFRA1 in the GFRA^{+}/UTF1^{-} Ap-d was twice as high as in GFRA1^{+}/UTF1^{+} Ap-d spermatogonia (Fig. 2H).

Proliferative activity of human Ap-d spermatogonia

To learn about the proliferative activity of the Ap-d spermatogonia, we stained tubule whole mounts for KI67, a marker of cells in all phases of the cell cycle except G0 (Birner et al., 2001; Gerdes et al., 1984; Scholzen and Gerdes, 2000). In this experiment, MAGEA4^{+}/KI67^{+}/KIT^{-} spermatogonia represent Ap-d spermatogonia in active cell cycle. KI67^{+} Ap-d spermatogonia were single, or in pairs or small groups of up to 6 cells (Fig. 3A). Only 5±2% of the Ap-d spermatogonia appeared positive for KI67 (Fig. 3B), indicating that 95±2% of the Ap-d spermatogonia are not in active cell cycle. Co-staining with MAGE-A4, GFRA1 and KI67 showed a comparable percentage of KI67^{+} Ap-d (6±2%), strongly suggesting that GFRA1 expression captures all the Ap-d spermatogonia that are in active cell cycle (Fig. S4).

Interestingly, UTF1^{+} Ap-d spermatogonia never stained for KI67 or for EdU (data not shown), indicating that UTF1^{+} cells were quiescent. Therefore, all KI67^{+} Ap-d were GFRA1^{High}/UTF1^{-}. When only 6% of the Ap-d spermatogonia are KI67^{+}, it can be calculated that about 15% of GFRA1+/UTF1^{-} (6% of 38%) are in active cell cycle.

These results suggest that early Ap-d spermatogonia are GFRA1 ^{High}/UTF1^{-}, and that these cells slowly proliferate. When UTF1 becomes expressed, these cells become quiescent and GFRA1 levels decrease.

Ap-d spermatogonia are mostly single cells and proliferate throughout the epithelial cycle

To study the topographical arrangement of Ap-d spermatogonia, we used the mitotic marker phosphohistone-H3 (PHH3) in whole-mounted seminiferous tubules. Mitosis takes only 2 h and as clones of Ap-d spermatogonia are not synchronized with each other, at any given moment few Ap-d spermatogonia will be in mitosis, allowing one to observe clonal sizes despite the high spermatogonial density. Mitotic Ap-d spermatogonia (MAGE-A4^{+}/KIT^{-}/PHH3^{+}) were rare and were mostly single cells (74±4%) and some pairs (26±4%). The

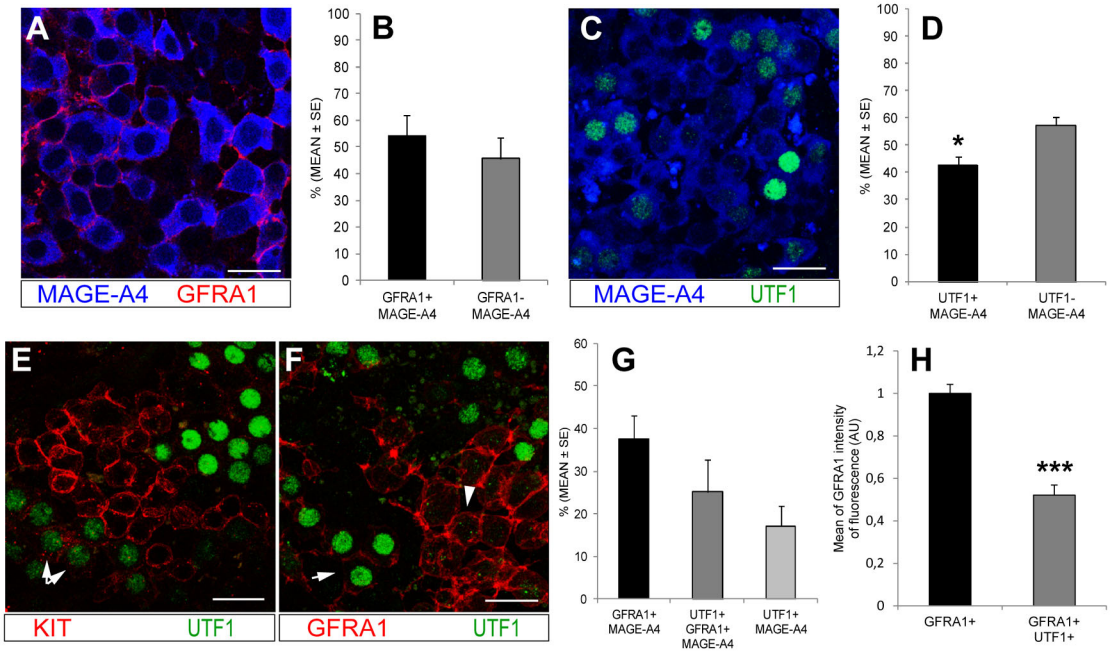

Fig. 2. Expression of GFRA1 and UTF1 in human spermatogonia. (A,B) Quantification of the relative proportion of GFRA1^{+} and GFRA1^{-} in human spermatogonia. (A) Representative images of intact seminiferous tubules co-stained for MAGE-A4 and GFRA1. (B) A total of 5850 GFRA1^{+}/MAGE-A4 and 5350 GFRA1^{-}/MAGE-A4 cells were scored in five samples. (C,D) Quantification of the relative proportion of UTF1^{+} and UTF1^{-} in human spermatogonia. (C) Representative images of intact seminiferous tubules co-stained for MAGE-A4 and UTF1. (D) A total of 3316 UTF1^{+}/MAGE-A4 and 4463 UTF1^{-}/MAGE-A4 cells were scored in three samples. *P<0.05 (Student's t-test). (E) Representative images of intact seminiferous tubules co-stained for KIT and UTF1. Double arrows indicate KIT^{+}/UTF1^{+} spermatogonia. KIT staining is weak in double-positive cells. (F,G) Quantification of the co-expression of GFRA1 and UTF1 among human spermatogonia. (F) Representative images of intact seminiferous tubules co-stained for MAGE-A4, GFRA1 and UTF1. Arrowhead indicates GFRA1^{+}/UTF1^{-}; arrow indicates GFRA1^{+}/UTF1^{+}. GFRA1 expression levels are higher in the GFRA1^{+}/UTF1^{-} Ap-d spermatogonia. (G) A total of 1467 GFRA1^{+}, 684 UTF1^{+} and 974 GFRA^{+}/UTF1^{+} cells were scored in three samples. (H) Data are from n=3 samples for a total of 240 cells analyzed. In each sample, 40 GFRA1/UTF1^{-} Ap-d and 40 GFRA1/UTF1^{+} Ap-d were analyzed. ***P<0.001 (Student's t-test). Scale bars: 20 µm.

Development (2017) 144, 3430-3439 doi:10.1242/dev.150284

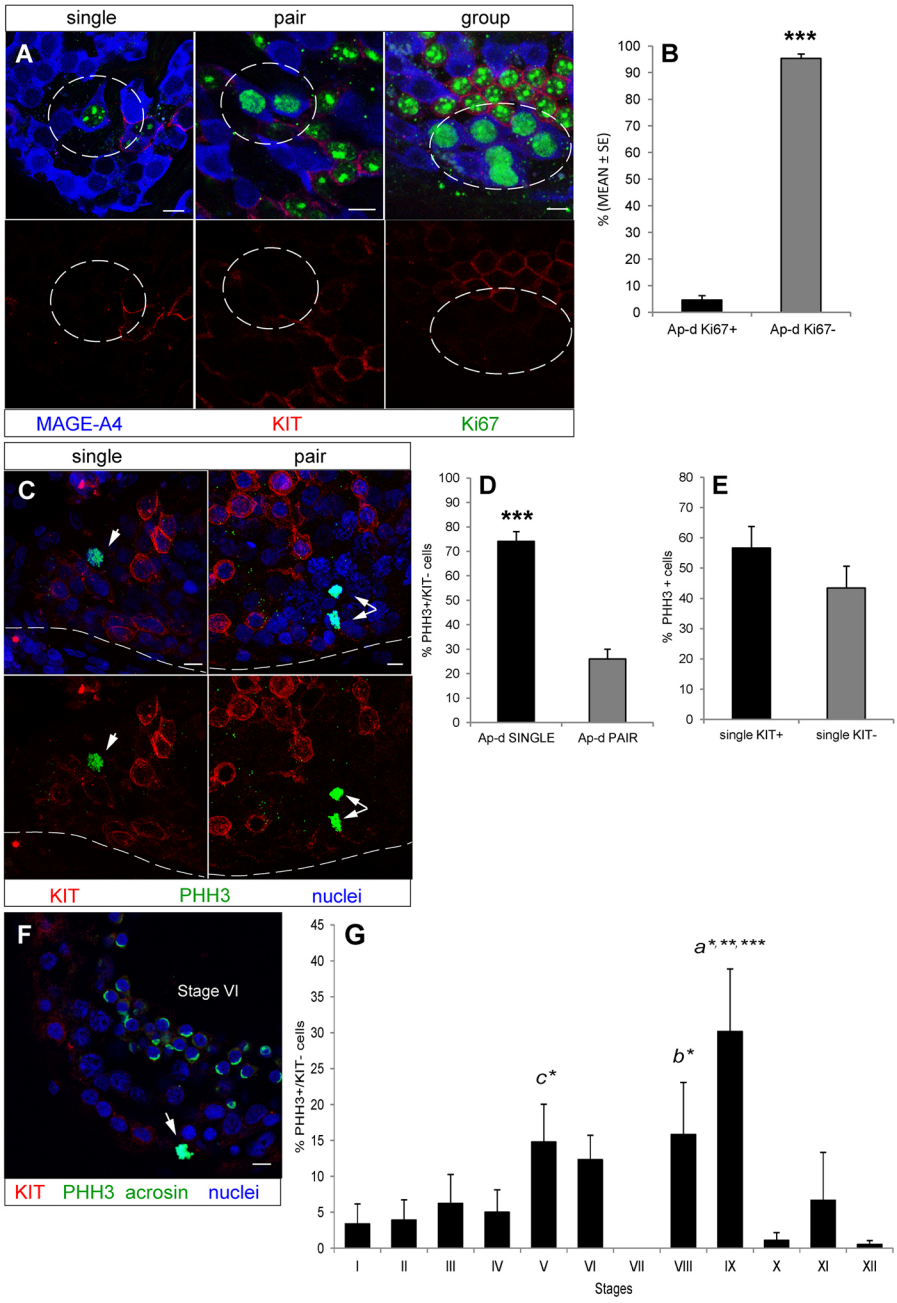

Fig. 3. Kinetics of human Ap-d spermatogonia. (A,B) Proliferation index of Ap-d. (A) Representative images of intact seminiferous tubules co-stained for KI67 to detect proliferating cells, MAGE-A4 and KIT. Dashed circles show a single (left), a pair (center) and a group (right) of KI67$^+$ Ap-d (MAGE-A4$^+$/KIT$^-$). (B) Quantification of proliferation index in three samples. A total of 102 KI67$^+$ Ap-d were scored out of 2235 Ap-d. ***P<0.001 (Student's t-test). (C,D) Quantification of the relative proportion of single and paired Ap-d (KIT$^-$/MAGE-A4$^+$/PHH3$^+$). (C) Representative images of intact seminiferous tubules co-stained for PHH3 to detect mitotic spermatogonia, for MAGE-A4 and for KIT. Single arrows indicate a single Ap-d; double arrows indicate a paired Ap-d. Dashed lines indicate the outline of the seminiferous tubules. (D) Relative proportion of single and paired Ap-d and 12 KIT$^-$ pairs were scored in five samples. ***P<0.001 (Student's t-test). (E) Quantification of the relative proportion of single Ap-d (KIT$^-$/MAGE-A4$^+$/PHH3$^+$) and single B (KIT$^+$/MAGE-A4$^+$/PHH3$^+$) spermatogonia. A total of 37 KIT$^-$ and 55 KIT$^+$ single cells were scored in five samples. (F,G) Distribution of mitotic Ap-d during the cycle of the seminiferous epithelium. (F) Representative images of formalin-fixed testis section stained for PHH3 to detect mitotic cells, KIT a marker of B spermatogonia and acrosin to visualize the epithelial stage. Nuclei are stained with TO-PRO-3. Single arrow indicates mitotic Ap-d at stage VI. (G) Histogram showing percentage of mitotic Ap-d (PHH3$^+$/KIT$^-$) per stage. A total of 64 PHH3$^+$/KIT$^-$ spermatogonia were counted in six samples. ^{a}*P<0.05 stage IX versus stage V, VI and VIII; ^{a}**P<0.005 stage IX versus III and XI; ^{a}***P<0.001 stage IX versus I, II, IV, X and XII; ^{b}*P<0.05 stage VIII versus X and XII; ^{c}*P<0.05 stage V versus X and XII. Scale bars: 10 µm.

pairs may either be two single Ap-d spermatogonia that coincidentally entered mitosis simultaneously or a true pair of Ap-d spermatogonia connected by an intercellular bridge (Fig. 3C,D). No chains of mitotic Ap-d spermatogonia were observed. This indicates that, in humans, most, if not all, Ap-d spermatogonia are single cells. Apparently, human undifferentiated spermatogonia do not, or rarely, form pairs and chains of cells as frequently occurs in rodents. Therefore, it will be mostly single Ap-d spermatogonia that differentiate into B spermatogonia. Single KIT$^+$/PHH3$^+$ cells, that should represent the division of the first generation of B spermatogonia, were observed. In response to the differentiation into B spermatogonia of some Ap-d spermatogonia, a comparable number of Ap-d spermatogonia should divide to replenish the cells lost to differentiation. Indeed, the number of dividing single KIT$^-$/PHH3$^+$ Ap-d spermatogonia was comparable with that of single KIT$^+$/PHH3$^+$ B spermatogonia (43±7% versus 57±7%, Fig. 3E).

We then asked whether divisions of Ap-d occur during particular stages of the epithelial cycle. In testis sections, mitotic spermatogonia were made clearly visible by immunofluorescent staining for PHH3 and for KIT, while epithelial stages were made visible by acrosin co-staining (Muciaccia et al., 2013). Again, mitotic figures of the KIT$^-$ Ap-d spermatogonia were rare (Fig. 3F). In samples from six donors, 64 KIT$^-$ mitoses of Ap-d spermatogonia were found that were spread throughout the epithelial stages, although numbers tended to be highest during stage IX (Fig. 3G). Hence, Ap-d spermatogonia proliferate throughout the epithelial cycle.

Three generations of human differentiating type B spermatogonia

In mammals, successive generations of differentiating spermatogonia divide synchronously during specific stages of the epithelial cycle. Generally, the number of peaks of mitotic spermatogonia during the

Development (2017) 144, 3430-3439 doi:10.1242/dev.150284

epithelial cycle equals the number of generations of differentiating spermatogonia. To reassess this number in the human, we used the 12-stage classification of the epithelial cycle (Muciaccia et al., 2013) and triple immunofluorescent staining of testis sections for acrosin to distinguish epithelial stages, for PHH3 to detect mitoses and for KIT to detect B spermatogonia. In total, 260 KIT^+ mitoses were observed in sections of six donors (Fig. 4A). Clear peaks of mitotic activity of KIT^+ mitotic spermatogonia were found in epithelial stages IX, II/III and V/VI, indicating that in the human there are three generations of differentiating spermatogonia (Fig. 4B). As in primates, differentiating spermatogonia are named B spermatogonia, these should be called B1, B2 and B3 spermatogonia, respectively. Our observations suggest that most, if not all, B spermatogonia are formed by differentiation of single Ap-d spermatogonia. When the B1 spermatogonia are singles, the B2 spermatogonia will be pairs and the B3 spermatogonia will be chains of four that will divide into chains of eight preleptotene spermatocytes.

During spermatogenesis, germ cells in the differentiation pathway form clones of cells that after division remain connected by intercellular bridges and move through the cell cycle synchronously. We analyzed the topographical arrangement of clones of mitotic B spermatogonia in tubule whole mounts fluorescently stained for KIT and PHH3 (Fig. 4C). Mitotic clones of B1, B2 and B3 spermatogonia were always found in groups ranging from three to 32 cells in which sometimes singles, pairs and larger clones could be distinguished (Fig. 4D). This indicates that relatively frequently, multiple clones of B spermatogonia synchronously traverse the cell cycle, causing them to enter mitosis simultaneously.

The regulation of human differentiating spermatogonial numbers

The number of three generations of B spermatogonia is higher than the one generation previously suggested by Clermont (Clermont, 1966b) but is still surprisingly low compared with the five to six generations of differentiating type spermatogonia observed in other mammals. We hypothesized that the number of human B spermatogonial divisions is downregulated, possibly because of the exceptionally high spermatogonial density. We therefore asked whether all B spermatogonia are in active cell cycle and analyzed

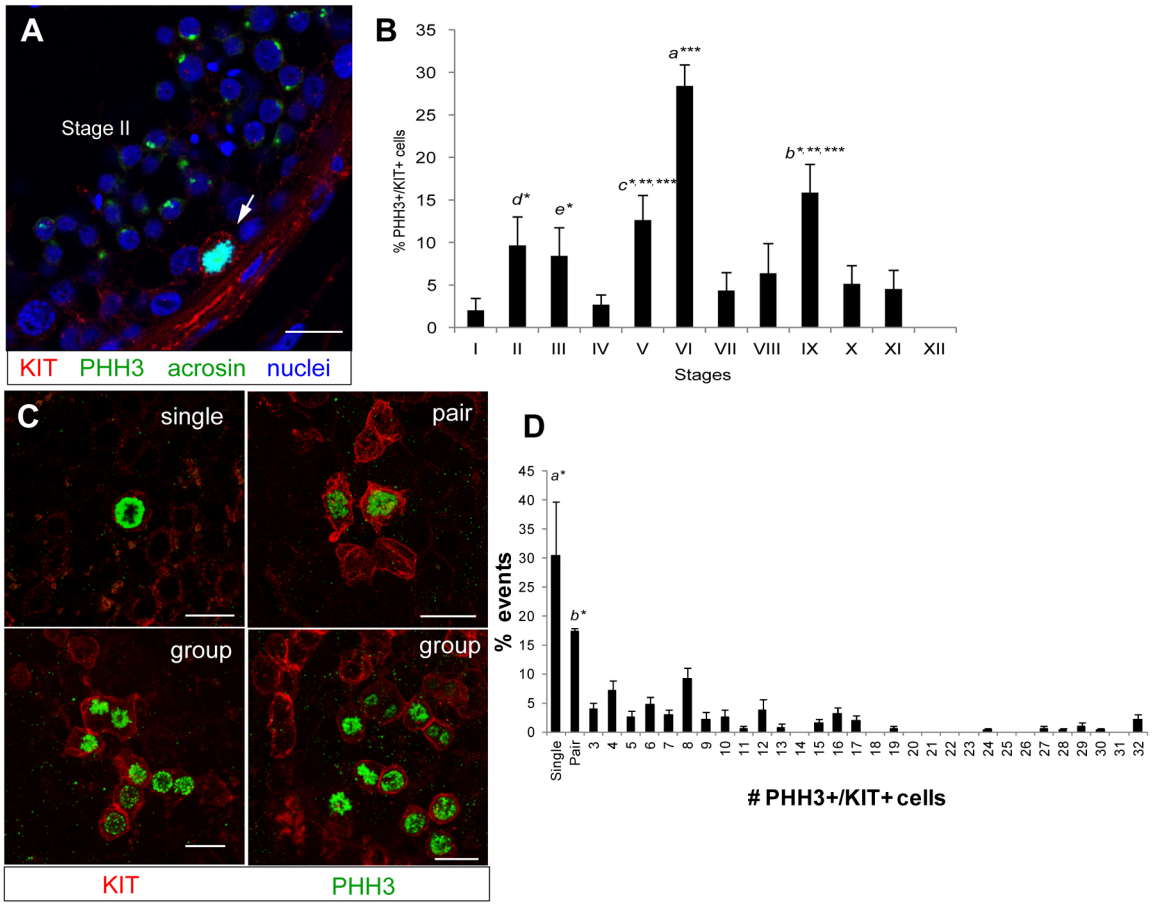

Fig. 4. Kinetics of human B spermatogonia. (A,B) Distribution of mitotic B spermatogonia during the cycle of the seminiferous epithelium. (A) Representative images of formalin-fixed testis sections stained for PHH3, KIT and acrosin to visualize the epithelial stage. Nuclei were stained with TO-PRO-3. Single arrow indicates mitotic B spermatogonia at stage II. (B) Histogram showing the percentage of mitotic B spermatogonia ($PHH3^+/KIT^+$) per stage. A total of 260 $PHH3^+/KIT^+$ spermatogonia were counted in six samples. $^{a***}P<0.001$ stage VI versus all other stages; $^{b***}P<0.001$ stage IX versus stages I, IV and XII; $^{b**}P<0.005$ stage IX versus stages VII, X and XI; $^{b*}P<0.05$ stage IX versus stages III and VIII; $^{c***}P<0.001$ stage V versus stage XII; $^{c**}P=0.05$ stage V versus stage I; $^{c*}P<0.05$ stage V versus stages IV, VII, X and XI; $^{d*}P<0.05$ stage II versus stages I and XII; $^{e*}P<0.05$ stage III versus stage XII. (C,D) Topographical arrangement of clones of mitotic B spermatogonia. (C) Intact seminiferous tubules co-stained for PHH3 and KIT. Representative images of single B spermatogonia, and pairs and groups of $PHH3^+$ B spermatogonia. (D) Relative frequencies of single B spermatogonia, and pairs and groups of 3-32 mitotic B spermatogonia in intact seminiferous tubules. A total of 260 $PHH3^+/KIT^+$ cells were scored in six samples. $^{a*}P<0.05$ single versus all others except pair; $^{b*}P<0.05$ pair versus all others except single. Scale bars: 20 µm.

Development (2017) 144, 3430-3439 doi:10.1242/dev.150284

the expression of KI67 (Fig. 5A). To our surprise, only 55±10% of the B spermatogonia were KI67$^+$, suggesting that almost half of human B spermatogonia are out of the cell cycle (Fig. 5B). Similar results were obtained using a different KI67 antibody (data not shown).

In rodents, all generations of differentiating spermatogonia are continuously proliferating. To verify that KI67 is a good spermatogonial proliferation marker, we studied KI67 expression in mouse differentiating type spermatogonia. Examining long stretches of seminiferous tubules, KIT$^+$ spermatogonia negative for KI67 were never observed, confirming that in the mouse all differentiating spermatogonia are in active cell cycle (Fig. S5). This finding supports the validity of using KI67 expression to study the proliferative activity of human differentiating spermatogonia and our conclusion that a considerable number of human B spermatogonia are not in the cell cycle. The proliferation of human differentiating type spermatogonia is apparently downregulated.

Furthermore, after each of the subsequent divisions, the number of B spermatogonia should double and consequently also the numbers of mitotic spermatogonia in the peaks. In contrast, the second mitotic peak is not higher than the first peak, and the third peak of mitotic B3 spermatogonia also does not seem to include twice the number of mitotic B2 spermatogonia. To study whether apoptosis could be the reason for the low numbers of mitotic B spermatogonia, we performed TUNEL staining to detect apoptotic cells. Indeed, apoptotic cells were detected on the basal lamina in between MAGE-A4$^+$ spermatogonia (Fig. 5C) and KIT$^+$ spermatogonia (Fig. 5D), making apoptosis a probable cause of the low peaks of mitotic B spermatogonia.

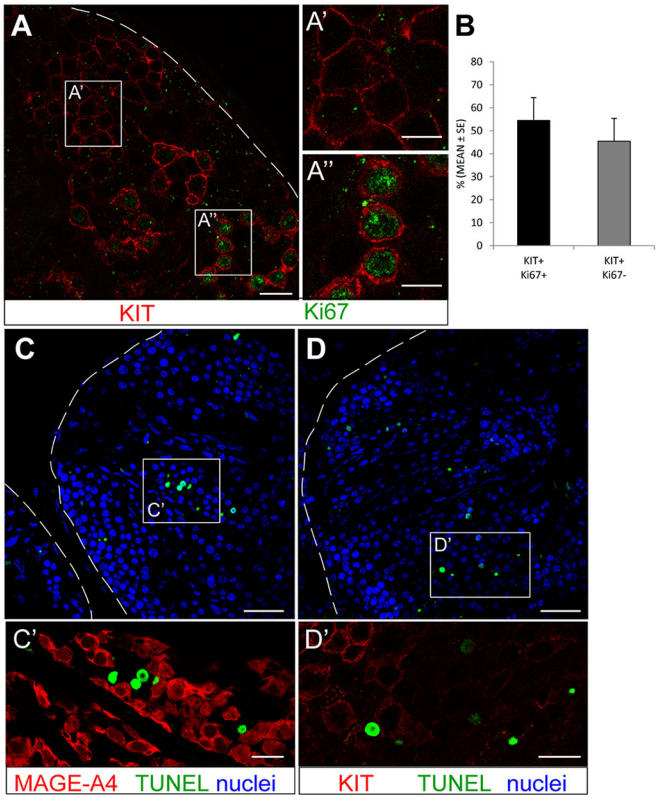

Fig. 5. Regulation of human differentiating spermatogonia. (A,B) Proliferation index of B spermatogonia. (A) Representative images of intact seminiferous tubules co-stained for KI67 and KIT. (B) A total of 742 Ki67$^+$/KIT$^+$ and 633 Ki67$^-$/KIT$^+$ cells were scored in three samples. (C,D) TUNEL assay on human seminiferous tubules. (C) Representative images of intact seminiferous tubules co-stained for TUNEL, MAGE-A4 and TO-PRO-3. An enlargement of the boxed area is shown in C′. (D) Representative images of intact seminiferous tubules co-stained for TUNEL, KIT and TO-PRO-3. An enlargement of the boxed area is shown in D′. Dashed lines indicate the outline of the seminiferous tubules. Scale bars: 10 µm in A′,A″; 20 µm in A,C′,D′; 50 µm in C,D.

DISCUSSION

Viewing whole mounts of human seminiferous tubules, one sees a surprisingly high density of spermatogonia with a highly variable morphology, which makes it impossible to distinguish spermatogonial subtypes. However, immunofluorescent staining for GFRA1, UCH-L1, UTF1 and KIT allowed us to discern sequential subpopulations of Ap-d spermatogonia. Furthermore, the regulation of B spermatogonial proliferation appeared to be more elaborate than in other mammalian species. The results led to the development of a novel model for steady state kinetics of human spermatogonia.

It proved impossible to reliably subdivide undifferentiated spermatogonia into Ap and Ad spermatogonia in tubule whole mounts, too many cells have an ‘in between’ morphology, suggesting a gradual transition from Ap to Ad spermatogonia. In monkey spermatogenesis, cells that are also intermediate between Ap and Ad spermatogonia have been described and these were called A-transition (At) (Fouquet and Dadoune, 1986) or A-unclassified (Aunc) (Simorangkir et al., 2005). Furthermore, Ehmcke and Schlatt reported that, in primates, 25 to 50% of the A spermatogonia cannot be unequivocally characterized as Ap or Ad (Ehmcke and Schlatt, 2006). We decided not to subdivide Ap-d spermatogonia on basis of their nuclear morphology but on the expression of marker proteins.

Our results show that all human spermatogonial cell types express MAGE-A4 and that 37% of the spermatogonia express KIT and are therefore B spermatogonia. The remaining KIT− spermatogonia are Ap-d spermatogonia that stain for UCHL1 with a small overlap of cells staining weakly for UCLH1 and KIT that are likely in transition between Ap-d and B (Fig. 6).

In line with our previous results, most Ap-d spermatogonia express the GDNF receptor GFRA1 (Grisanti et al., 2009) (Fig. 6). In this, human Ap-d spermatogonia resemble those of the rhesus monkey in which all Ap-d spermatogonia express GFRA1 (Hermann et al., 2009). Only 6% of the GFRA1$^+$ Ap-d spermatogonia also express KI67, indicating that most of these cells are not in cell cycle. The transcription factor UTF1 is also expressed in a majority 56±4% of Ap-d and in very few B spermatogonia. UTF1 has been associated with the capacity of human embryonal carcinoma cells to differentiate in response to RA (Lin et al., 2012). Interestingly, in rodents the differentiation of A_{al} spermatogonia into differentiating type spermatogonia is induced by RA. A few UTF1$^+$ B spermatogonia weakly express UTF1 and also weakly express KIT. In view of the suggested role of UTF1 in RA action, it seems likely that the UTF1 weak B spermatogonia are in the process of losing UTF1 and acquiring KIT expression during the differentiation of Ap-d into B spermatogonia. Remarkably, UTF1$^+$ spermatogonia never co-stain for KI67, indicating that UTF1 expressing Ap-d spermatogonia are quiescent. All proliferative activity in the compartment of Ap-d spermatogonia is therefore carried out by GFRA1$^+$/UTF1$^-$ cells. Interestingly, the expression level of GFRA1 in GFRA1$^+$/UTF1$^-$ Ap-d is twofold higher than in GFRA1$^+$/UTF1$^+$ Ap-d spermatogonia. This indicates that the acquisition of UTF1 expression is an important step in the development of Ap-d spermatogonia as they become both quiescent and GFRA1^{Low}.

Development (2017) 144, 3430-3439 doi:10.1242/dev.150284

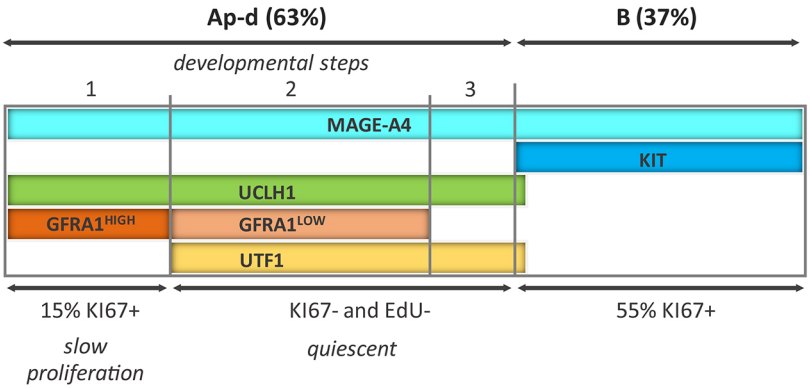

Fig. 6. Proposed scheme for human spermatogonial multiplication and stem cell renewal, based on marker protein expression and mitotic activity of the cells. The SSCs reside in the GFRA1^{High}/UTF1^{-} Ap-d spermatogonia and differentiating cells are recruited from GFRA1^{Low}/UTF1^{+} Ap-d spermatogonia. Note the very low proliferative activity of the Ap-d.

Based on our results, we suggest the following picture for the human spermatogonial compartment. At the start of the human spermatogenic lineage, there is a pool of GFRA1^{High}/UTF1^{-} Ap-d comprising 32% of all Ap-d spermatogonia, which in the normal epithelium slowly proliferate (Fig. 6). During each epithelial cycle, some cells in the GFRA1^{+}/UTF1^{-} pool start to express UTF1 and become part of a pool of quiescent UTF1^{+}/GFRA1^{Low} Ap-d, comprising 56% of all Ap-d spermatogonia. At some point, GFRA1 expression is lost and the cells become part of a compartment of GFRA1^{-}/UTF1^{+} spermatogonia that may be competent to differentiate into B1 spermatogonia, as evidenced by the occurrence of cells that are weakly stained for both UTF1 and the differentiation marker KIT (Fig. 6). In contrast to UTF1, UCH-L1 is expressed in all Ap-d spermatogonia and, similarly to UTF1, UCH-L1 expression is lost in B spermatogonia. Recently, a single cell RNA-seq experiment was carried out on human spermatogonia (Neuhaus et al., 2017). Heterogeneous expression profiles were found but the results did not yet lead to a better insight into spermatogonial behavior in humans. However, when the results can be related to our initial scheme based on GFRA1, UTF1 and KIT expression, the single-cell RNA-seq approach may well lead to a further refinement of our proposed scheme. Our data obtained using the marker PHH3, which labels the relatively rare mitotic Ap-d spermatogonia in whole mounts of seminiferous tubules, show that at least the majority of human Ap-d spermatogonia are single cells. Some pairs of Ap-d spermatogonia were also found, but we do not know whether these are true pairs or mitotic singles that happen to be in the vicinity of one another. Comparable numbers of single mitotic Ap-d spermatogonia and single mitotic B spermatogonia were found. Single Ap-d spermatogonia apparently differentiate into single B spermatogonia that subsequently enter the cell cycle and comparable numbers of single Ap-d spermatogonia divide to replenish the Ap-d spermatogonia lost to differentiation.

During the human epithelial cell cycle, there are three peaks of mitotic activity of B spermatogonia indicating the presence of three generations of B spermatogonia: B1, B2 and B3. As the B1 spermatogonia are single cells and probably some paired cells, this means that the spermatocytes consist of clones of 8-16 cells compared with about 1000 in mice (Russell et al., 1990). This difference will be smaller in monkeys in which 4-5 spermatogonial divisions have been found (Clermont and Antar, 1973; de Rooij and Russell, 2000; Ehmcke et al., 2005; Fouquet and Dadoune, 1986). We found three generations of B spermatogonia and not one generation as previously described (Clermont, 1966b). In our analysis we used the novel 12-stage classification and not the six-stage classification of the human epithelial cycle used by Clermont (Muciaccia et al., 2013). The shorter duration of each stage in the novel classification allowed a more detailed analysis of mitotic peaks.

Only few of the GFRA1^{High}/UTF1^{-} Ap-d spermatogonia stain for KI67 and are therefore in active cell cycle. This begs the question of how much proliferative activity is needed to replenish the Ap-d lost to differentiation? Using our data, we can give a possible answer. During the steady state, i.e. once every epithelial cycle, B1 spermatogonia should be formed by differentiation of Ap-d spermatogonia. We showed that 37 out of every 100 spermatogonia are B spermatogonia. When there is no apoptosis of B spermatogonia, one-seventh of these cells (about five spermatogonia) should be B1 spermatogonia (1B1-2B2-4B3, so B1 spermatogonia compose one-seventh of the total). We also found that only 15 out of every 100 GFRA1^{High}/UTF1^{-} Ap-d spermatogonia are in active cell cycle. Therefore, during the steady state, about five out of 15 (one-third) GFRA1^{High}/UTF1^{-} Ap-d spermatogonia, should divide once during one epithelial cycle to replenish Ap-d spermatogonia lost to differentiation. This suggests that, on average, the GFRA1^{High}/UTF1^{-} Ap-d only divide once every three epithelial cycles, i.e. one and a half months, and that these cells are out of the cell cycle for prolonged periods of time. In comparison, in rodents and sheep, A_s, A_{pr} and A_{al} spermatogonia divide two or three times per epithelial cycle (Lok and de Rooij, 1983; Lok et al., 1983; Tegelenbosch and de Rooij, 1993). Furthermore, as indicated above, in this calculation five UTF1^{+} Ap-d become B spermatogonia (i.e. 7% of UTF1^{+} Ap-d spermatogonia) each epithelial cycle. This suggests that per epithelial cycle, UTF1^{+} Ap-d only have a chance of about 7% to leave the pool of quiescent Ap-d spermatogonia. Apparently, in each epithelial cycle only a small proportion of the Ap-d can make the step to differentiating type spermatogonia; therefore, on average, the UTF1^{+} cells may stay quiescent for about 7-8 months.

It is conceivable that the long periods of time during which both GFRA1^{High}/UTF1^{-} and GFRA1^{Low}/UTF1^{+} Ap-d spermatogonia are not in cell cycle brings along a gradual transition from the Ap to the Ad morphology. When this is indeed the case for both these cell types, the distinction between Ap and Ad spermatogonia clearly does not relate to different cell types, and the latter would explain why over time little progress has been made in understanding primate spermatogonial behavior. Nuclear rarefaction zones, as seen in typical Ad spermatogonia, have also been described in undifferentiated spermatogonia in mice and the Chinese hamster, and were found to be to restricted to cells in G0/G1 phase (de Rooij, 1973; Lok et al., 1982). Nothing can be said as yet about whether or not the acquisition of Ad morphology influences the likelihood of GFRA1^{High}/UTF1^{-} cells entering the cell cycle or the responsiveness of the GFRA1^{Low}/UTF1^{+} cells to a differentiation stimulus. In rodents, the chains of A-aligned spermatogonia become

Development (2017) 144, 3430-3439 doi:10.1242/dev.150284

quiescent at about stage II, at which point they become capable of responding to induction of differentiation by retinoic acid (Endo et al., 2015). Therefore, quiescence of the cells may be related to competence of the cells towards induction of differentiation, and UTF1 may be involved in inducing quiescence of these cells.

Although, in mouse, all differentiating type spermatogonia express KI67, only 55% of human B spermatogonia do so. This indicates that, at any given moment, almost half of human B spermatogonia are not in active cell cycle. This may occur in two ways: (1) B spermatogonia have a low random chance to enter the cell cycle; or (2) they are inhibited to proliferate during particular time periods of the epithelial cycle. The first possibility does not seem attractive as it does not explain the occurrence of only three mitotic peaks, in fact one would not even expect the presence of peaks. The second option offers the possibility for the epithelium to restrict the number of B spermatogonial divisions by inducing quiescence of these cells during specific epithelial stages. Such a regulatory pathway governing the number of differentiating spermatogonial generations will have to be confirmed in further studies. In rodents, differentiating spermatogonia are always in active cell cycle. Apparently, in humans and possibly in other primates, where generally about four or five generations of B spermatogonia are described, there is a mechanism to control the number of generations of differentiating type spermatogonia.

In addition, there may be density-related apoptosis of B spermatogonia that causes a reduction of B spermatogonial mitoses during the second and third mitotic peaks. Indeed, as assessed by TUNEL staining, spermatogonial apoptosis does take place. Apoptosis of differentiating type spermatogonia is observed in all non-primate mammals and serves to regulate cell density. In areas with many differentiating spermatogonia, many of these cells will enter apoptosis; in areas with only few of these cells, few or none will do so. This ensures an even distribution of preleptotene spermatocytes over the tubule basal lamina (de Rooij and Janssen, 1987; de Rooij and Lok, 1987).

In humans and in some monkeys (Wistuba et al., 2003), areas that are in the same epithelial stage are only small, leading to the presence of multiple stages in the cross-section of one tubule. Our data provide several reasons for this phenomenon. In humans, only single spermatogonia and perhaps a few pairs of Ap-d spermatogonia differentiate, instead of the chains of four to 16 A_{al} spermatogonia in rodents. Furthermore, in humans there are fewer generations of differentiating spermatogonia to follow than in rodents, i.e. three instead of six, making a further eightfold difference. Both reasons will lead to much smaller tubule areas being in the same epithelial stage in humans than in rodents.

Thus far, both Ap and Ad spermatogonia have been considered to be stem cells. Our results suggest that the SSCs will reside in the population of the Ap-d spermatogonia that are $GFRA1^{High}/UTF1^{-}$. However, one has to be wary of assigning a stem cell role to all these cells, because in the mouse it has recently been shown that only some of the single As spermatogonia are true stem cells, while the rest of the single spermatogonia likely have a limited self-renewal capacity (Aloisio et al., 2014; Chan et al., 2014; Helsel et al., 2017; Komai et al., 2014; Oatley et al., 2011). Interestingly, mouse true SSCs have recently been found to be $GFRA1^{High}$ (Helsel et al., 2017), suggesting that in humans the 32% of Ap-d spermatogonia that are $GFRA1^{High}/UTF1^{-}$ are also, or at least include, SSCs. This will need further studies.

In conclusion, GFRA1 and UTF1 are marker proteins that enable one to subdivide the human spermatogonial compartment in a more meaningful way than by using nuclear morphology. We suggest that the development of Ap-d spermatogonia can be subdivided into three steps: the earliest Ap-d spermatogonia that are $GFRA1^{High}$ and include SSCs; the Ap-d spermatogonia that start to express UTF1, followed by a reduction in GFRA1 expression and quiescence; and finally the spermatogonia in which GFRA1 expression stops and the cells become competent to differentiate into B spermatogonia (Fig. 6). The study of additional markers may well add further details to this process of Ap-d development and SSC renewal. Furthermore, our results will be particularly helpful in the interpretation of single RNA-seq data. In addition, it will facilitate the understanding of cases of male infertility due to spermatogonial failure and help the development of treatment strategies. In this respect, when $UTF1^{+}$ Ap-d are analogous to A_{al} spermatogonia, it is interesting that the latter cells can already be induced to differentiate in stages II to VI by injection of retinoic acid (Endo et al., 2015).

MATERIALS AND METHODS

Human testis sample collection

Testicular biopsies were used from heart-beating organ donors (n=15 samples from 19 to 75 years of age) at the hospital Policlinico Umberto I (Rome, Italy). For each donor, the free and informed consent of the family concerned, was obtained. The Ethical Committee of the hospital approved the use of human material according to national guidelines for organ donation as issued by the Italian Ministry of Public Health. Biopsies were collected as previously described (Muciaccia et al., 2013). From each donor, representative samples from different parts of the testis were collected. After collection, the biopsies were transported in ice-cold phosphate buffered saline (PBS) (Sigma-Aldrich) to the laboratory and processed within 1 h. Biopsies were routinely fixed in Bouin's fixative and embedded in paraffin wax but in some instances samples were fixed in 10% buffered formalin (Sigma-Aldrich) or 4% paraformaldehyde (PFA) (Electron Microscopy Sciences). Some biopsies were left unfixed and used for short-term culture.

In order to check the integrity of the tissue and the preservation of spermatogenesis, Bouin-fixed samples were paraffin wax-embedded, sections stained with Mayer's Hematoxylin and Eosin (Sigma-Aldrich), and analyzed. All the samples included in this study showed well-preserved testicular tissue and a normal spermatogenesis without any sign of fibrosis or inflammation.

EdU incorporation and detection

Unfixed testicular fragments obtained from biopsies were cultured in αMEM medium containing 4 mM glutamine, 1% non essential amino acids, 2% penicillin/streptomycin, 0.08% gentamicin, 15 mM HEPES (pH 7.7) and 10 µM EdU (5-ethynyl-2′-deoxyuridine) at 34°C in 5% CO_2 for 2 h and 30 min (all reagents were from Thermo Fisher Scientific). After incubation, fragments were gently dissociated to obtain isolated seminiferous tubules and fixed in 4% paraformaldehyde at 4°C for 4 h. EdU detection was performed by following the protocol of the Click-iT EdU Imaging Kits (Thermo Fisher Scientific). Following EdU detection, tubules were used to detect various antigens using whole-mount immunofluorescence.

Immunofluorescence

Sections (5 µm) of formalin-fixed samples were processed in a microwave oven for antigen retrieval in citrate buffer (pH 6.0; DAKO). To reduce nonspecific background signal, sections were incubated with 1 M glycine (Sigma-Aldrich) and subsequently with 1% BSA (Sigma-Aldrich) and 5% normal donkey serum (Jackson Laboratories Immuno Research). Subsequently, sections were incubated overnight at 4°C with appropriate primary antibodies. The primary antibodies used are listed in Table S1. After the washes, the sections were incubated with species-specific secondary antibodies for 2 h at room temperature. All secondary ALEXA488- and Cy3-conjugated antibodies were from Jackson Immuno Research. At the end, the nuclei were counterstained with TO-PRO-3 Iodide (642/661) (T3605, Thermo Fisher Scientific) and the slides closed with Vectashield mounting medium (Vector Laboratories). Pictures were acquired using a Leica TCS SP2 confocal microscope with a 40× oil immersion objective.

Development (2017) 144, 3430-3439 doi:10.1242/dev.150284

For whole-mount immunofluorescence, seminiferous tubules were disentangled from testicular biopsies and immediately fixed in 4% PFA at 4°C for 4 h. Fixed tubules were permeabilized with 0.5% Triton X100, treated with 1 M glycine for 1 h, and with 0.1% Triton X-100, 1% BSA and 5% normal donkey serum in PBS overnight at 4°C. The following day, tubules were washed in 1% BSA, 0.1% Triton X-100 in PBS (three times for 30 min) and incubated overnight at 4°C with appropriate primary antibodies (Table S1).

The following day, tubules were washed as above and incubated with species-specific secondary antibodies conjugated to Alexa 488-, Cy3- or Cy5-conjugated fluorochromes for 2 h at room temperature. Primary and secondary antibodies were diluted in 1% BSA and 0.1% Triton X-100 in PBS. After the secondary antibody, tubules were washed as above and nuclei were stained with TO-PRO-3. Tubules were mounted onto slides using Vectashield mounting medium and observed using a Leica TCS SP2 confocal microscope with 40× oil immersion objective or an inverted Olympus IX83 microscope with 60× water immersion objective.

Whole-mount immunofluorescence analysis of adult mouse seminiferous tubules was performed as previously described (Corallini et al., 2006). Fixed seminiferous tubules were incubated with primary antibodies (Table S1) at 4°C for 16 h under constant shaking. After washing, the tubules were incubated with the species-specific conjugated secondary antibodies for 2 h at room temperature. Nuclei were stained with TO-PRO-3.

For quantification of GFRA1 expression levels, intact seminiferous tubules from three different testis samples were co-stained for GFRA1 and UTF1. *Z*-stacks were acquired using a Leica TCS SP2 confocal microscope at 1 µm increments between *z*-slices using a 40× oil immersion objective. All images were taken under the same conditions. The mean fluorescence intensity was quantified using LAS AF Software. For each donor, 80 cells were selected and analyzed from several seminiferous tubules.

TUNEL assay

The TUNEL (TdT-mediated X-dUTP nick end labeling) assay on human intact seminiferous tubules was performed as previously described (Hamer et al., 2003) using the In Situ Cell Death Detection Kit, Fluorescein (Roche Diagnostic) with minor modifications. The PFA-fixed tubules were permeabilized with 1% Triton X-100 (Sigma-Aldrich) for 1 h at room temperature. After two washes in PBS some tubules were treated with RNase-Free DNase Set (Qiagen) for 20 min at room temperature as a positive control. Tubules were then briefly washed in PBS and incubated in TUNEL mix (enzyme plus label) at 37°C for 2 h. As negative control, some tubules were incubated only with the TUNEL label (without enzyme) at 37°C for 2 h. Finally, tubules were washed three times with PBS and were used for detection of different antigens using whole-mount immunofluorescence.

Imaging and spermatogonial quantification

In order to quantify the relative proportion of Ap-d subsets and the proliferation index of Ap-d and B spermatogonia, intact seminiferous tubules from at least three different testis samples were co-stained for relevant antibodies. Owing to the convoluted nature of human seminiferous tubules, in order to image the entire spermatogonial layer, *z*-stacks were acquired using Leica TCS SP2 confocal microscope with a 40×oil immersion objective or an inverted Olympus IX83 microscope with 60× water immersion objective. For each testis sample, ten fields (187.5×187.5 µm) were randomly selected from at least three different seminiferous tubules. For each field, confocal *z*-stacks were acquired (at 1 µm increments between *z*-slices).

To estimate the size and the frequency of $PHH3^+/KIT^+$ groups, five different samples were used. In each sample, stained tubules were individually analyzed from the beginning to the end in order to detect $PHH3^+/KIT^+$ cells. *Z*-stacks (at 1 µm increments between *z*-slices) were then acquired for each field containing labeled cells.

In order to estimate the frequency of mitotic Ap-d and B spermatogonia, testis sections from six samples were co-stained for relevant antibodies and analyzed using Leica TCS SP2 confocal microscope with a 40× oil immersion objective. $PHH3^+$ spermatogonia were rare and therefore several sections from each sample had to be analyzed to reach an adequate number of observations. All quantifications were performed on stored microphotographs using the LAS AF Software or Fiji/ImageJ Software.

Statistical analysis

All quantitative data are shown as the mean±s.e.m. To define the significance of the differences between two groups, data were analyzed using a *t*-test. To compare many groups, data were analyzed using one-way analysis of variance (ANOVA) followed by a post hoc Fisher LSD Method. The significance level was fixed at $P=0.05$.

Acknowledgements

We are grateful to Stefania De Grossi and Tiziana Menna for excellent technical support, and to Dr G. Spagnoli (Basel, Switzerland) for kindly providing the mouse anti-MAGE-A4 antibody. We acknowledge the Centre for Life Nano Science of the Istituto Italiano di Tecnologia for providing microscopy facilities, and we thank Dr S. De Panfilis for assistance in using the instruments.

Competing interests

The authors declare no competing or financial interests.

Author contributions

Conceptualization: S.D.P., M.S., D.G.d.R., E.V.; Methodology: S.D.P., D.G.d.R., E.V.; Validation: S.D.P., D.G.d.R., E.V.; Formal analysis: S.D.P., M.S., D.G.d.R., E.V.; Investigation: S.D.P., R.S., S.F., B.M., V.E., C.B., M.S., D.G.d.R., E.V.; Resources: B.P.B., F.N., G.S.; Data curation: S.D.P.; Writing - original draft: S.D.P., D.G.d.R., E.V.; Writing - review & editing: S.D.P., D.G.d.R., E.V.; Funding acquisition: E.V.

Funding

This work was supported by grants from Sapienza Università di Roma (Ateneo 2014-2016) and from Istituto Pasteur-Fondazione Cenci Bolognett to E.V.

Supplementary information

Supplementary information available online at
http://dev.biologists.org/lookup/doi/10.1242/dev.150284.supplemental

References

Aloisio, G. M., Nakada, Y., Saatcioglu, H. D., Peña, C. G., Baker, M. D., Tarnawa, E. D., Mukherjee, J., Manjunath, H., Bugde, A., Sengupta, A. L. et al. (2014). PAX7 expression defines germline stem cells in the adult testis. *J. Clin. Invest.* **124**, 3929-3944.

Aubry, F., Satie, A.-P., Rioux-Leclercq, N., Rajpert-De Meyts, E., Spagnoli, G. C., Chomez, P., De Backer, O., Jégou, B. and Samson, M. (2001). MAGE-A4, a germ cell specific marker, is expressed differentially in testicular tumors. *Cancer* **92**, 2778-2785.

Birner, P., Ritzi, M., Musahl, C., Knippers, R., Gerdes, J., Voigtländer, T., Budka, H. and Hainfellner, J. A. (2001). Immunohistochemical detection of cell growth fraction in formalin-fixed and paraffin-embedded murine tissue. *Am. J. Pathol.* **158**, 1991-1996.

Chan, F., Oatley, M. J., Kaucher, A. V., Yang, Q.-E., Bieberich, C. J., Shashikant, C. S. and Oatley, J. M. (2014). Functional and molecular features of the Id4+ germline stem cell population in mouse testes. *Genes Dev.* **28**, 1351-1362.

Clermont, Y. (1966a). Renewal of spermatogonia in man. *Am. J. Anat.* **118**, 509-524.

Clermont, Y. (1966b). Spermatogenesis in man. A study of the spermatogonial population. *Fertil. Steril.* **17**, 705-721.

Clermont, Y. (1969). Two classes of spermatogonial stem cells in the monkey (Cercopithecus aethiops). *Am. J. Anat.* **126**, 57-71.

Clermont, Y. and Antar, M. (1973). Duration of the cycle of the seminiferous epithelium and the spermatogonial renewal in the monkey Macaca arctoides. *Am. J. Anat.* **136**, 153-165.

Corallini, S., Fera, S., Grisanti, L., Falciatori, I., Muciaccia, B., Stefanini, M. and Vicini, E. (2006). Expression of the adaptor protein m-Numb in mouse male germ cells. *Reproduction* **132**, 887-897.

de Rooij, D. G. (1973). Spermatogonial stem cell renewal in the mouse. I. Normal situation. *Cell Tissue Kinet.* **6**, 281-287.

de Rooij, D. G. and Janssen, J. M. (1987). Regulation of the density of spermatogonia in the seminiferous epithelium of the Chinese hamster: I. Undifferentiated spermatogonia. *Anat. Rec.* **217**, 124-130.

de Rooij, D. G. and Lok, D. (1987). Regulation of the density of spermatogonia in the seminiferous epithelium of the Chinese hamster: II. Differentiating spermatogonia. *Anat. Rec.* **217**, 131-136.

de Rooij, D. G. and Russell, L. D. (2000). All you wanted to know about spermatogonia but were afraid to ask. *J. Androl.* **21**, 776-798.

Ehmcke, J. and Schlatt, S. (2006). A revised model for spermatogonial expansion in man: lessons from non-human primates. *Reproduction* **132**, 673-680.

Ehmcke, J., Luetjens, C. M. and Schlatt, S. (2005). Clonal organization of proliferating spermatogonial stem cells in adult males of two species of non-human primates, Macaca mulatta and Callithrix jacchus. *Biol. Reprod.* **72**, 293-300.

Development (2017) 144, 3430-3439 doi:10.1242/dev.150284

Ehmcke, J., Wistuba, J. and Schlatt, S. (2006). Spermatogonial stem cells: questions, models and perspectives. *Hum. Reprod. Update* **12**, 275-282.

Endo, T., Romer, K. A., Anderson, E. L., Baltus, A. E., de Rooij, D. G. and Page, D. C. (2015). Periodic retinoic acid-STRA8 signaling intersects with periodic germ-cell competencies to regulate spermatogenesis. *Proc. Natl. Acad. Sci. USA* **112**, E2347-E2356.

Fouquet, J. P. and Dadoune, J. P. (1986). Renewal of Spermatogonia in the Monkey (Macaca Fascilularis). *Biol. Reprod.* **35**, 199-207.

Gerdes, J., Lemke, H., Baisch, H., Wacker, H. H., Schwab, U. and Stein, H. (1984). Cell cycle analysis of a cell proliferation-associated human nuclear antigen defined by the monoclonal antibody Ki-67. *I. Immunol.* **133**, 1710-1715.

Grisanti, L., Falciatori, I., Grasso, M., Dovere, L., Fera, S., Muciaccia, B., Fuso, A., Berno, V., Boitani, C., Stefanini, M. et al. (2009). Identification of spermatogonial stem cell subsets by morphological analysis and prospective isolation. *Stem Cells* **27**, 3043-3052.

Hamer, G., Roepers-Gajadien, H. L., Gademan, I. S., Kal, H. B. and De Rooij, D. G. (2003). Intercellular bridges and apoptosis in clones of male germ cells. *Int. J. Androl.* **26**, 348-353.

Helsel, A. R., Yang, Q.-E., Oatley, M. J., Lord, T., Sablitzky, F. and Oatley, J. M. (2017). ID4 levels dictate the stem cell state in mouse spermatogonia. *Development* **144**, 624-634.

Hermann, B. P., Sukhwani, M., Simorangkir, D. R., Chu, T., Plant, T. M. and Orwig, K. E. (2009). Molecular dissection of the male germ cell lineage identifies putative spermatogonial stem cells in rhesus macaques. *Hum. Reprod.* **24**, 1704-1716.

Hermann, B. P., Sukhwani, M., Hansel, M. C. and Orwig, K. E. (2010). Spermatogonial stem cells in higher primates: are there differences from those in rodents? *Reproduction* **139**, 479-493.

Huckins, C. (1971). The spermatogonial stem cell population in adult rats. I. Their morphology, proliferation and maturation. *Anat. Rec.* **169**, 533-557.

Johnson, L. (1994). A new approach to study the architectural arrangement of spermatogenic stages revealed little evidence of a partial-wave along the length of human seminiferous tubules. *J. Androl.* **15**, 435-441.

Komai, Y., Tanaka, T., Tokuyama, Y., Yanai, H., Ohe, S., Omachi, T., Atsumi, N., Yoshida, N., Kumano, K., Hisha, H. et al. (2014). Bmi1 expression in long-term germ stem cells. *Sci. Rep.* **4**, 6175.

Lin, C.-H., Yang, C.-H. and Chen, Y.-R. (2012). UTF1 deficiency promotes retinoic acid-induced neuronal differentiation in P19 embryonal carcinoma cells. *Int. J. Biochem. Cell Biol.* **44**, 350-357.

Lok, D. and de Rooij, D. G. (1983). Spermatogonial multiplication in the Chinese hamster. III. Labelling indices of undifferentiated spermatogonia throughout the cycle of the seminiferous epithelium. *Cell Tissue Kinet.* **16**, 31-40.

Lok, D., Weenk, D. and de Rooij, D. G. (1982). Morphology, proliferation, and differentiation of undifferentiated spermatogonia in the Chinese hamster and the ram. *Anat. Rec.* **203**, 83-99.

Lok, D., Jansen, M. T. and de Rooij, D. G. (1983). Spermatogonial multiplication in the Chinese hamster. II. Cell cycle properties of undifferentiated spermatogonia. *Cell Tissue Kinet.* **16**, 19-29.

Meng, X., Lindahl, M., Hyvonen, M. E., Parvinen, M., de Rooij, D. G., Hess, M. W., Raatikainen-Ahokas, A., Sainio, K., Rauvala, H., Lakso, M. et al. (2000). Regulation of cell fate decision of undifferentiated spermatogonia by GDNF. *Science* **287**, 1489-1493.

Muciaccia, B., Boitani, C., Berloco, B. P., Nudo, F., Spadetta, G., Stefanini, M., de Rooij, D. G. and Vicini, E. (2013). Novel stage classification of human spermatogenesis based on acrosome development. *Biol. Reprod.* **89**, 60.

Neuhaus, N., Yoon, J., Terwort, N., Kliesch, S., Seggewiss, J., Huge, A., Voss, R., Schlatt, S., Grindberg, R. V. and Schöler, H. R. (2017). Single-cell gene expression analysis reveals diversity among human spermatogonia. *Mol. Hum. Reprod.* **73**, 79-90.

Oatley, M. J., Kaucher, A. V., Racicot, K. E. and Oatley, J. M. (2011). Inhibitor of DNA binding 4 is expressed selectively by single spermatogonia in the male germline and regulates the self-renewal of spermatogonial stem cells in mice. *Biol. Reprod.* **85**, 347-356.

Rowley, M. J. and Heller, C. G. (1971). Quantitation of cells of seminiferous epithelium of human testis employing Sertoli cell as a constant. *Z. Zellforsch. Mikrosk. Anat.* **115**, 461-472.

Russell, L. D., Ettlin, R. A., Hikim, A. P. S. and Clegg, E. D. (1990). *Histological and Histopathological Evaluation of the Testis*. Clearwater, FL: Cache River Press.

Scholzen, T. and Gerdes, J. (2000). The Ki-67 protein: from the known and the unknown. *J. Cell Physiol.* **182**, 311-322.

Schrans-Stassen, B. H. G. J., van de Kant, H. J. G., de Rooij, D. G. and van Pelt, A. M. M. (1999). Differential expression of c-kit in mouse undifferentiated and differentiating type A spermatogonia. *Endocrinology* **140**, 5894-5900.

Simorangkir, D. R., Marshall, G. R., Ehmcke, J., Schlatt, S. and Plant, T. M. (2005). Prepubertal expansion of dark and pale type A spermatogonia in the rhesus monkey (Macaca mulatta) results from proliferation during infantile and juvenile development in a relatively gonadotropin independent manner. *Biol. Reprod.* **73**, 1109-1115.

Simorangkir, D. R., Marshall, G. R. and Plant, T. M. (2009). A re-examination of proliferation and differentiation of type A spermatogonia in the adult rhesus monkey (Macaca mulatta). *Hum. Reprod.* **24**, 1596-1604.

Singh, D., Paduch, D. A., Schlegel, P. N., Orwig, K. E., Mielnik, A., Bolyakov, A. and Wright, W. W. (2017). The production of glial cell line-derived neurotrophic factor by human sertoli cells is substantially reduced in Sertoli cell-only testes. *Hum. Reprod.* **32**, 1108-1117.

Spinnler, K., Kohn, F. M., Schwarzer, U. and Mayerhofer, A. (2010). Glial cell line-derived neurotrophic factor is constitutively produced by human testicular peritubular cells and may contribute to the spermatogonial stem cell niche in man. *Hum. Reprod.* **25**, 2181-2187.

Tegelenbosch, R. A. J. and de Rooij, D. G. (1993). A quantitative study of spermatogonial multiplication and stem cell renewal in the C3H/101 F1 hybrid mouse. *Mutat. Res.* **290**, 193-200.

Tokunaga, Y., Imai, S., Torii, R. and Maeda, T. (1999a). Alterations of basal lamina of the seminiferous epithelium during the seasonal suppression of spermatogenesis in the Japanese monkey (Macaca fuscata). *Acta Histochem. Cytochem.* **32**, 359-368.

Tokunaga, Y., Imai, S., Torii, R. and Maeda, T. (1999b). Cytoplasmic liberation of protein gene product 9.5 during the seasonal regulation of spermatogenesis in the monkey (Macaca fuscata). *Endocrinology* **140**, 1875-1883.

van Alphen, M. M., van de Kant, H. J. and de Rooij, D. G. (1988). Depletion of the spermatogonia from the seminiferous epithelium of the rhesus monkey after X irradiation. *Radiat. Res.* **113**, 473-486.

van den Boom, V., Kooistra, S. M., Boesjes, M., Geverts, B., Houtsmuller, A. B., Monzen, K., Komuro, I., Essers, J., Drenth-Diephuis, L. J. and Eggen, B. J. L. (2007). UTF1 is a chromatin-associated protein involved in ES cell differentiation. *J. Cell Biol.* **178**, 913-924.

von Kopylow, K., Kirchhoff, C., Jezek, D., Schulze, W., Feig, C., Primig, M., Steinkraus, V. and Spiess, A. N. (2010). Screening for biomarkers of spermatogonia within the human testis: a whole genome approach. *Hum. Reprod.* **25**, 1104-1112.

von Kopylow, K., Staege, H., Spiess, A.-N., Schulze, W., Will, H., Primig, M. and Kirchhoff, C. (2012). Differential marker protein expression specifies rarefaction zone-containing human A_{dark} spermatogonia. *Reproduction* **143**, 45-57.

Wistuba, J., Schrod, A., Greve, B., Hodges, J. K., Aslam, H., Weinbauer, G. F. and Luetjens, C. M. (2003). Organization of seminiferous epithelium in primates: relationship to spermatogenic efficiency, phylogeny, and mating system. *Biol. Reprod.* **69**, 582-591.